Journal of Engineering Mathematics 21: 3–16 (1987)

Loss of lift due to thickness for low-aspect-ratio wings in incompressible flow

S.S. Dodbele [1] & A. Plotkin [2]
[1] *Vigyan Research Associates, Inc., Hampton, VA, USA;* [2] *Department of Aerospace Engineering and Engineering Mechanics, San Diego State University, San Diego, CA 92182, USA*

Received 29 April 1986; accepted in revised form 3 October 1986

Abstract

The problem under consideration is a numerical study of the effects of thickness on lift for low-aspect-ratio wings in steady incompressible inviscid flow at moderate angles of attack. At these angles of attack the flow separates along the leading edge giving rise to a lift substantially higher than that computed by classical attached-flow potential theory. The problem is treated as a perturbation expansion in a small thickness parameter. The lifting elements of the flow are modeled using a nonlinear vortex-lattice method which replaces the leading and trailing-edge vortex sheets by segmented straight vortex filaments. The thickness elements of the flow are modeled with a mean-plane source distribution and a modification to the wing boundary conditions. Results are obtained for wings with biconvex and NACA 0012 sections which compare well with available experimental data. The important observation that the effect of thickness is to decrease the lift is made.

1. Introduction

At moderate to high angles of attack flow separates along the leading edge of a low-aspect-ratio delta wing resulting in a free shear layer. This free shear layer rolls up in a spiral fashion, just inboard of the leading edges, to form leading-edge vortex flow. The general nature of this separated flow is well understood having been the subject of several enlightening experimental investigations [1–6]. However, accurate theoretical prediction of the nonlinear effects is still being investigated as evidenced by numerous current journal articles and excellent reviews by Smith [7], Lamar and Campbell [8] and Hoeijmakers [9]. Among several methods [10–17] to compute vortex flows on three-dimensional wings the nonlinear vortex-lattice methods [14,16] are relatively simple and yield fairly decent aerodynamic coefficients. In these methods discrete line-vortex segments trail from the leading and the trailing edges. These vortices form the discrete representation of the roll-up of the leading-edge vortex sheet and the trailing wake sheet. The boundary conditions on the sheet surfaces are satisfied by aligning the segments parallel to the local flow direction, while simultaneously their strengths are determined by satisfying the wing boundary condition.

Very few investigations have been made to study the aerodynamic characteristics of delta wings with round leading edges. It is important to study this aspect in some more detail since one of the main effects of thickness on low-aspect-ratio delta wings is to decrease the aerodynamic lift.

Kulfan [18] has developed a concept for treating a round leading edge, where only a partial recovery of the suction force is achieved. The method can be used to predict the spanwise

development of the leading-edge vortices on highly swept wings with round-nose airfoils. Lan [12], using the quasi-vortex lattice method with suction analogy, * estimated the aerodynamic characteristics of round-leading-edge wings incorporating the effect of vortex breakdown. Lamar [8,19], using the vortex-lattice method with suction analogy, computed the aerodynamic coefficients of a round-leading-edge wing. But, using the suction analogy, one cannot predict the pressure and the velocity distributions. The higher-order panel method developed at Boeing by Johnson et al. [13] is the most sophisticated panel method for computing subsonic subcritical flow about configurations with free vortex sheets. Recently the method has been made to handle the cases of wing thickness, camber and twist [20]. But when the method was applied to the case of a flat wing with thickness, it produced larger pressure peaks than the experimental data. Gordon and Rom [17] have used the vortex-lattice method to calculate the aerodynamic characteristics of a series of delta wings with or without camber. They have developed a method based on the vortex-lattice method and panel source singularities to calculate the aerodynamic coefficients of thick wings with sharp leading edges.

Plotkin [21] has developed corrections to aerodynamic coefficients obtained from slender-wing theory for wings of vanishing aspect ratio with spanwise thickness and camber. Weber [22] has developed a second-order perturbation theory for wings of finite thickness and camber in incompressible attached flow. The flow field is represented by a distribution of sources and lifting singularities on the mean chord surface. Following her method, Sells [23] computed the steady, inviscid flow around thick wings at incidence.

The thickness effect is the focal point of the present paper. A method to study the effects of thickness on lift for triangular wings, which also gives the details of the flow, is studied here. In this method, sources and vortices are distributed on the mean surface of the thick wing and the nonlinear discrete-vortex technique is used to deal with the separated flow from the leading edges and the nonlinear wake from the trailing edge.

3. General formulation for wings with thickness at moderate angle of attack

Consider the steady incompressible flow of a uniform stream with speed U and at an angle of attack α past a delta wing with thickness. The flow over the wing is assumed to separate from the leading edge giving rise to leading-edge vortex flow and also there is a vortex sheet emanating from the trailing edge. The flow is assumed to be inviscid and irrotational outside the wing and the vortex sheets.

The leading-edge vortex is taken to be full span and the breakdown of the vortex systems at large angles of attack is not considered. A cartesian coordinate system is placed at the apex of the wing with the wing mean plane lying in the xy-plane. The xz-plane is a plane of symmetry. The thickness is assumed to be small compared to the wing-root chord C.

The flow outside the wing and its free vortex sheets is governed by Laplace's equation,

$$\nabla^2 \Phi = 0, \tag{1}$$

where Φ is the total velocity potential given by

$$\Phi = Ux \cos \alpha + Uz \sin \alpha + \phi \tag{2}$$

and ϕ is the disturbance velocity potential.

* The so-called suction analogy is based on the assumption that for flow separation along the leading edge, the suction force is recovered as a force rotated through 90° to act in the direction of the normal force.

For moderate α and small τ, the disturbance potential ϕ can be written as *

$$\phi = \phi_0 + \tau\phi_1 + O(\tau^2). \tag{3}$$

Let the wing boundary surface be defined by

$$0 = F(x, y, z) = z - \tau H(x, y). \tag{4}$$

We are seeking the solution of Laplace's equation (1) subject to the following conditions (a)–(d):

(a) The velocity is tangent to the wing surface. Therefore,

$$\nabla\Phi \cdot \nabla F = 0 \quad \text{on } F = 0 \tag{5}$$

where

$$\nabla\Phi = (U\cos\alpha + \phi_x, \phi_y, U\sin\alpha + \phi_z). \tag{6}$$

(b) There is no pressure jump across the wakes emanating from the leading edges and the trailing edges of the wing.

(c) The Kutta condition which requires finite velocity at the wing edges should be satisfied.

(d) The disturbance velocity, $\nabla\phi$, must vanish far from the wing and the wake surfaces.

The modeling of the perturbation flow field with a system of discrete vortex segments guarantees satisfaction of the conditions of incompressibility and irrotationality (equation (1)) and also ensures that the uniform stream is recovered far from the wing and the wakes. The strengths of the vortex segments are determined such that the rest of the conditions are satisfied.

Since we are considering symmetric wings and if $\tau Z_t(x, y)$ is the thickness function (thickness is $2\tau Z_t(x, y)$), we have

$$H(x, y) = \pm Z_t(x, y). \tag{7}$$

Combining equations (5) and (7) we get

$$(U\cos\alpha + \phi_x)(\pm\tau Z_{tx}) + \phi_y(\pm\tau Z_{ty}) - (\phi_z + U\sin\alpha) = 0 \quad \text{on } Z = \pm\tau Z_t. \tag{8}$$

It is assumed that the velocity potential and its derivatives can be expanded in Taylor series about the wing mean plane. The Taylor series expansions are used in the boundary condition given by equation (8) and after simplification, the following equation is obtained:

$$\pm\tau U\cos\alpha Z_{tx} \pm \tau Z_{tx}\{\phi_{0x}(x, y, 0\pm) + \tau[\phi_{1x}(x, y, 0\pm) \pm Z_t\phi_{0xz}(x, y, 0\pm)]\}$$

$$\pm\tau Z_{ty}\{\phi_{0y}(x, y, 0\pm) + \tau[\phi_{1y}(x, y, 0\pm) \pm Z_t\phi_{0yz}(x, y, 0\pm)]\}$$

$$-\phi_{0z}(x, y, 0\pm) - \tau[\phi_{1x}(x, y, 0\pm) \pm Z_t\phi_{0zz}(x, y, 0\pm)] - U\sin\alpha = O(\tau^2). \tag{9}$$

* This approach complements the investigation of Weber [22] for the attached-flow (small α) case.

Collecting terms of order 1 and τ, we get

$$\tau^0 : \phi_{0z}(x, y, 0\pm) = -U \sin\alpha, \tag{10}$$

$$\tau^1 : \phi_{1z}(x, y, 0\pm) = \pm U \cos\alpha Z_{tx} \pm Z_{tx}\phi_{0x}(x, y, 0\pm) \pm Z_{ty}\phi_{0y}(x, y, 0\pm) \mp Z_t\phi_{0zz}(x, y, 0\pm). \tag{11}$$

It follows from equation (10) that ϕ_0 is antisymmetric in z and ϕ_{0z} is symmetric in z in the neighborhood of the wing surface and ϕ_0 represents the velocity potential for the flow past a delta wing of infinitesimal thickness which we will refer to as the basic problem.

Now, consider equation (11). We can use the symmetry properties of ϕ_0 with respect to z to separate the velocity potential ϕ_1 into lifting (ϕ_{11}) and nonlifting (ϕ_{12}) parts,

$$\phi_1 = \phi_{11} + \phi_{12}, \tag{12}$$

where the lifting potential ϕ_{11} and the z-derivative of the nonlifting potential ϕ_{12} are antisymmetric in z in the neighborhood of the wing surface.

With the use of these symmetry properties and Laplace's equation, the first-order boundary condition for the lifting problem to be satisfied on the wing mean surface can be written as

$$\phi_{11z}(x, y, 0\pm) = \partial/\partial x\big(Z_t\phi_{0x}(x, y, 0+)\big) + \partial/\partial y\big(Z_t\phi_{0y}(x, y, 0+)\big). \tag{13}$$

The first-order thickness problem is then

$$\nabla^2\phi_{12} = 0, \tag{14}$$

$$\phi_{12z}(x, y, 0\pm) = \pm U \cos\alpha Z_{tx}, \tag{15}$$

$$\nabla\phi_{12} \to 0 \text{ at infinite distances.} \tag{16}$$

Note here that the wake conditions are absent for the thickness problem due to the symmetric nature of the velocity potential ϕ_{12} about the xy-plane. The thickness problem can be solved by distributing sources on the wing mean plane.

The complete first-order lifting problem is now given by

$$\nabla^2\phi_{1L} = 0 \tag{17}$$

where

$$\phi_{1L} = \phi_0 + \tau\phi_{11} \tag{18}$$

and is subject to the conditions

$$\text{(a)}\quad \phi_{1Lz}(x, y, 0\pm) = -U \sin\alpha + \tau\big\{\partial/\partial x\big(Z_t\phi_{0x}(x, y, 0+)\big) + \partial/\partial y\big(Z_t\phi_{0y}(x, y, 0+)\big)\big\}; \tag{19}$$

$$\text{(b)}\quad \nabla\phi_{1L}\cdot\nabla F_W = -\nabla(Ux\cos\alpha + Uz\sin\alpha + \tau\phi_{12})\cdot\nabla F_W \quad \text{on } F_W(x, y, z) = 0; \tag{20}$$

(c) there is no pressure jump across the wakes emanating from the leading edges and the trailing edges of the wing;

(d) the Kutta condition which requires finite velocity at the wing edges should be satisfied;

(e) the disturbance velocity $\nabla\phi_{1L}$ must vanish far from the wing and the wake surfaces.

Since the function $F_w(x, y, z) = 0$ representing the leading-edge sheet and the trailing-edge sheet is a nonlinear unknown function and has to be obtained as part of the solution (as in the case of the basic problem), a close examination of equation (20) reveals that the first-order problem and the basic problem cannot be solved separately and added together to obtain the complete first-order lifting solution. The first-order lifting problem has to be solved along with the basic problem.

It is important to note that the above formulation of the problem for the thick wing is independent of the solution technique.

4. Delta wing with thickness at moderate angles of attack

4.1. The discrete vortex model

The wing mean plane is divided into a system of triangular and quadrilateral panels by equally-spaced chordwise lines and equally-spaced spanwise lines (see Fig. 1). Each panel is aerodynamically represented by bound vortex segments. For the panels adjacent to the leading edge, the bound vortex segment starting from the quarter chord of the panel root chord goes up to the mid-span length of the panel along the quarter-chord line and is directed along the perpendicular to the leading edge. With reference to the Kutta condition, the velocity at the

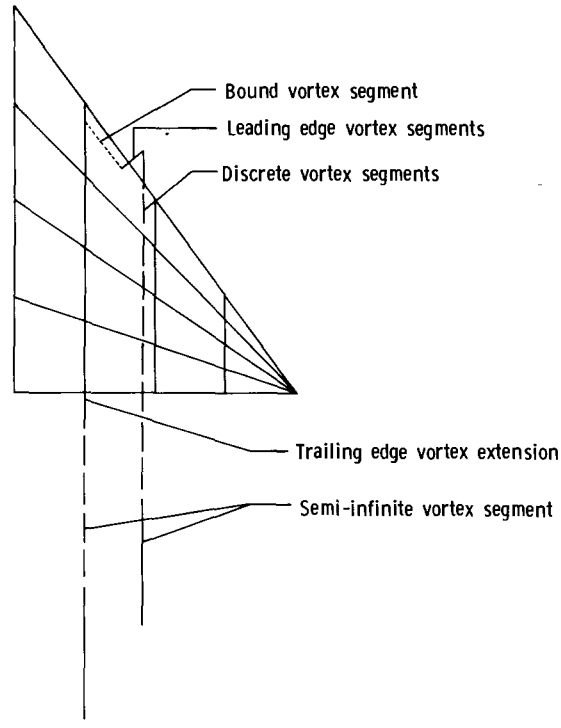

Fig. 1. Discrete vortex system.

leading edge is only infinite at the point at which the bound vortex crosses the edge and, following the discussion given in [14], the vortex segment is arranged to emerge out of the wing perpendicular to the leading edge. The vortex filament arrangement for a leading-edge panel is shown in Fig. 1.

Free vortex segments representing the leading-edge separation start from an extension of the bound vortex segment beyond the leading edge. The bound vortex is connected to a semi-infinite vortex segment through a number of vortex segments. The other end of the bound vortex continues downstream in the wing mean plane parallel to the x-axis until it extends beyond the trailing edge, where it is connected to a semi-infinite vortex line through a number of smaller vortex segments (see Fig. 1).

The interior panels are modeled by horseshoe vortices whose legs extend beyond the trailing edge and are connected to semi-infinite vortex lines far downstream again through a number of short vortex segments. On any of these interior panels, the bound vortex segment lies along the quarter-chord line of the panel. The control point (downwash point) is chosen to be at the intersection of the mid-span line and the three-quarter chord line. The basic problem was solved by the discrete vortex-lattice method in which the discrete vortex segments model the lifting elements of the flow. The leading-edge vortex sheets are modeled again by discrete vortex segments. The problem is solved iteratively by satisfying the wing and wake boundary conditions on the wing and the wake surfaces at the selected control points.

4.2. Solution to the thickness problem

The solution to the thickness problem given by equations (14–16) is given in [24]. The perturbation velocity potential ϕ_{12} is given by the following expression:

$$\phi_{12}(x, y, z) = -(1/2\pi)\iint_A \left(U \cos \alpha Z_{tx'}(x', y')/r\right) \mathrm{d}x' \, \mathrm{d}y' \tag{24}$$

where $r = [(x - x')^2 + (y - y')^2 + z^2]^{1/2}$.

Physically, equation (24) states that the flow due to thickness can be represented by a source sheet over the wing mean surface (A) with the source strength per unit area being twice the quantity $U \cos \alpha Z_{tx}$.

4.3. Solution to the lifting problem

The first-order lifting problem is essentially the same as the basic problem of flow around an infinitesimally thin wing with leading-edge separation with the following differences:

(1) In the neighborhood of the leading edge, segments are modeled differently;
(2) The boundary conditions to be satisfied on the wing mean surface include the effect of the thickness, (see equation (19));
(3) The effect of the sources is to be considered while calculating the downstream ends of the finite vortex segments representing the leading-edge wake and the trailing-edge wake.

Other than these additional features, the solution technique for the first-order lifting problem is essentially the same as that for the basic problem.

In the leading-edge region the vortex-segment extension is modeled in the following way:

(a) *Leading-edge region for sharp-edged wings.* For a wing with a sharp leading edge, since the flow separates at the leading edge, the streamlines emerge tangential to the lower surface at

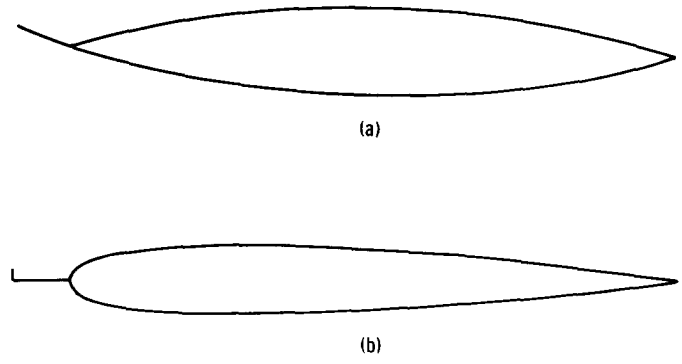

Fig. 2. Leading-edge vortex-segment extension: (a) biconvex; (b) NACA 0012.

the leading edge (for positive α). Calculations were done by choosing the first leading edge extension to be tangential to the bottom surface (see Fig. 2a).

(b) *Leading-edge region for round-edged wings.* In the case of wings with round leading edges with small thickness parameter τ, we do not know precisely the location of the separation line. To within the accuracy of the modeling of the leading-edge separation by the discrete vortex-segment method, we can take the separation line to be along the leading edge. To simulate the flow leaving tangent to the leading edge, the leading-edge vortex-segment extension was taken first perpendicular to the leading edge but in the wing mean plane and then turned around 90 degrees in the direction normal to the wing mean surface (see Fig. 2b).

Since the flow model cannot accurately represent the regular velocity field in the neighborhood of the leading edge, the sophistication of the above leading-edge extensions needs some justification. For both sharp and round-edge wings, calculations were also made with extensions in the wing mean plane. For the sharp-edged wings, both models yield reasonable force coefficients and it is not clear which one yields the best overall comparisons with experiment. For the round-edged wings, the model used in the paper gave substantially better agreement with experimental results for the lift coefficient for the NACA 0012 section. It was the judgment of the authors to use the leading-edge extension models which most closely modeled the physics since no other criterion for the choice was apparent.

The details of the length of the leading-edge extensions, the initial shape of the vortex segments modelling the wakes, and the orientation of the vortex segments are discussed at length in [26].

Once the initial positions of the leading-edge vortex segments and the trailing-edge vortex segments are given, the velocity at each control point on the wing mean surface can be calculated using the Biot-Savart law. If $\mathbf{V}_m$ is the velocity induced at each control point due to the vortex segments on the wing and in the wake, we have

$$\mathbf{V}_m = \sum_{n=1}^{N} \mathbf{A}_{mn}\Gamma_n, \quad m = 1, \ldots, N, \tag{25}$$

where $\mathbf{A}_{mn}$ are known vector quantities, N is the total number of wing panels, and Γ_n are the unknown vortex strengths.

The boundary condition to be satisfied on the wing mean surface is given by equation (19):

$$-U \sin \alpha + \tau\left[\partial/\partial x\{Z_t\phi_{0x}(x, y, 0+)\} + \partial/\partial y\{Z_t\phi_{0y}(x, y, 0+)\}\right] = \sum_{n=1}^{N} \mathbf{A}_{mn} \cdot \mathbf{k}\Gamma_n \tag{26}$$

where **k** is a unit vector in the z-direction. For a wing of infinitesimal thickness the terms in the bracket will be absent.

Equation (26) is a set of N linear algebraic simultaneous equations and can easily be solved for the unknowns Γ_n by standard algorithms.

Once the circulation distribution Γ_n is known, the condition that each vortex segment in the leading and trailing-edge wakes be aligned with the local velocity vector is used to calculate the downstream ends of the finite vortex segments. In this way the kinematic and dynamic boundary conditions on the vortex sheets are satisfied. The location of the downstream end of each vortex segment is calculated from the equation

$$\mathbf{r}_{j+1} = \mathbf{r}_j + \left[\mathbf{V}_j l_j / |\mathbf{V}_j|\right] \tag{27}$$

where $\mathbf{r}_j$, l_j and $\mathbf{V}_j$ are, respectively, the position vector of the upstream end, and the length and velocity at the control point (upstream end) of the jth vortex segment at the end of, say, the nth iteration. These quantities are used to obtain the downstream end of the jth vortex segment at the end of the nth iteration to go in as the input for the $(n+1)$st iteration. While calculating the velocities at the control points (upstream end points) of the vortex segments we have to take into consideration the influences of the entire vortex system (bound and free) and the velocities induced by the source distribution. For computational efficiency, the continuous source distribution is discretized and distributed on a convenient number of constant source panels. The velocity due to those source panels is calculated as in Woodward [25] and details are given in Dodbele [26,27]. Once the position vectors of the ends of the free vortex segments are determined the contribution of these wake vortex segments along with the contribution of the bound vortex segments are used to obtain corrected influence coefficients to be used in equation (25) again. Thus the iteration process alternates between the control points on the wing and the control points on the vortex sheets. The process is said to have converged when the maximum of the absolute difference between the x, y and z coordinates representing the vortex-sheet shape from two successive iterations is less than a certain prescribed tolerance. With the vortex strengths thus determined, the pressure distribution on each of the panels and the overall aerodynamic coefficients are determined.

4.4. Results and discussion

Aerodynamic characteristics are obtained for a delta wing of $AR = 1.0$ having a 12% biconvex airfoil section and a surface generated by radial straight lines from the tips. This wing has a constant biconvex shape with a constant thickness/chord ratio across the span. Gordon and Rom [17] have obtained aerodynamic characteristics for this biconvex section wing. They do not consider the terms involving the thickness in the boundary condition to be satisfied on the wing mean surface and also they have taken the first leading-edge extension in the wing mean plane. In Fig. 3 lift coefficients obtained by the present method are indicated along with the theoretical results obtained by Gordon and Rom [17] and the experimental results obtained by Peckham [2]. From the figure we see that the lift coefficients obtained by the present method for the biconvex section wing are in good agreement with the experimental results at higher angles of attack.

Each of the wing halves was discretized by dividing the root chord and the semi-span into n equal divisions each. The full wing then has $2n^2$ panels. Convergence studies were undertaken which showed that 50 panels ($n = 5$) were sufficient to get the lift coefficient to within one percent of its converged value. Also, eight iterations were needed for the lift-coefficient convergence.

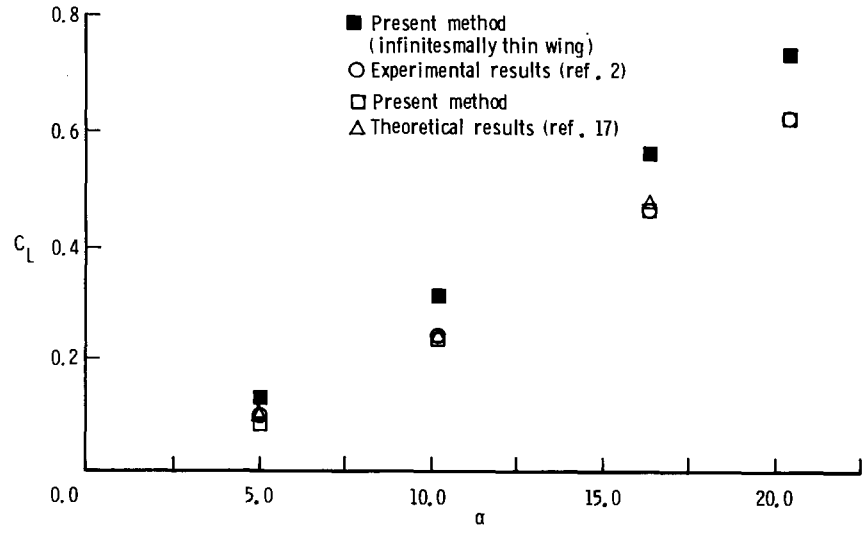

Fig. 3. Lift coefficients for a biconvex section wing of $AR = 1.0$ and thickness ratio 12%.

Figure 3 also presents lift coefficients obtained for the biconvex wing and also the thin wing with the same aspect ratio 1.0. This figure confirms the experimental observation that the effect of thickness is to decrease the lift. Wing thickness affects the solution in two ways: (a) through the boundary conditions to be satisfied on the wing mean surface, see equation (19), and (b) the location of the vortex segments modeling the leading and the trailing-edge sheet shapes, see equation (20). The contribution of the thickness terms in the boundary condition is quite small compared to the dominant term $-U \sin \alpha$. This would appear to justify the choice of Gordon and Rom [17] to neglect these thickness terms in their analysis.

The spanwise load distribution at a chordwise position of $0.75C$ is computed and presented in Fig. 4 along with the experimental results. Though the theoretical pressure curve is underpredicting it is showing the right trend. It is closer to the experimental data in the inboard section. In the same figure the results obtained by Gordon and Rom [17] at the chordwise station $0.73C$ are also plotted. It is noted that the vortex-lattice method is expected to calculate more accurately overall forces than pressure distributions.

Next, aerodynamic coefficients for a NACA 0012 section wing with $AR = 4/\sqrt{3}$ were computed and are presented in Fig. 5. For this wing experimental results are available [6]. Kulfan [18], Lamar [8,19] and Lan [12], independently, have obtained the lift coefficients for this wing at a number of angles of attack. All the three investigators have used the suction analogy to predict the vortex lift.

For round-leading-edge wings at lower angles of attack, attached flow or partial leading-edge vortex flow separation occurs and hence the present computational procedure is not expected to give very accurate results since full span leading edge separation is assumed. In Fig. 5, the lift coefficients obtained agree very well with the experimental results at higher angles of attack. The lift coefficients predicted are within about 2.5% of the experimental results. At large angles of attack, since the present computational procedure does not incorporate the breakdown feature of the vortex system, the method is not expected to give accurate results. Nevertheless, the results obtained by the present method are in good agreement at $\alpha = 20°$. Figure 5 also presents lift coefficients obtained by the theoretical method developed by Lamar [8]. Results obtained by Lamar are a little higher than the experimental results at lower angles and the gap tends to widen at higher angles of attack. Results obtained by Lan [12] (not shown in the figure) were also a little higher than the experimental results but very close to the results

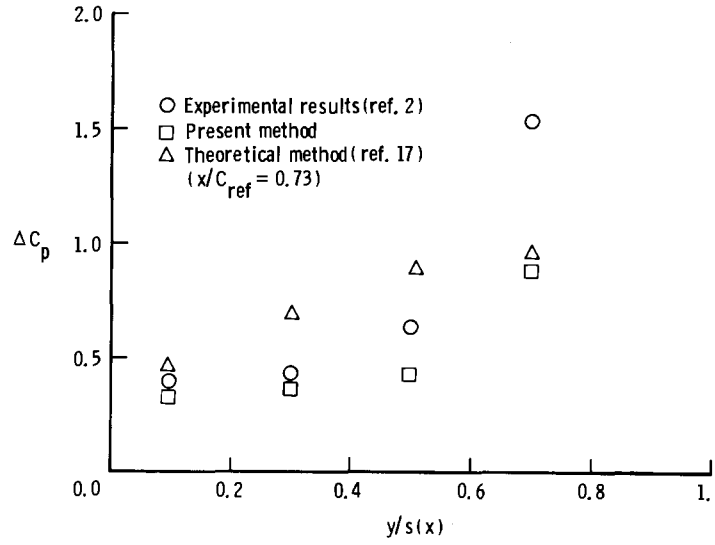

Fig. 4. Spanwise load distribution for a biconvex section wing of $AR = 1.0$, with thickness ratio 12% at $\alpha = 20.4°$, $x/C_{ref} = .75$.

obtained by Lamar. Lift coefficients obtained by Kulfan [18] (not shown in the figure) seem to be very close to the experimental results [6]. When the vortex breakdown effect was included in Lan's [12] method the lift coefficients seemed to agree very well with the experimental results.

In Fig. 5 lift coefficients obtained by the present theory for the NACA 0012 section delta wing and a very thin delta wing, both with $AR = 4/\sqrt{3}$ are compared. Here, again, it is confirmed that the effect of thickness is to decrease the lift.

Until now we have been discussing the effect of thickness on lift for delta wings with full-span leading-edge vortex separation at moderate angles of attack. For delta wings with sharp leading edges flow separates all along the leading edge at all angles of attack. But in the case of wings with round leading edges there could be part-span separation at certain low

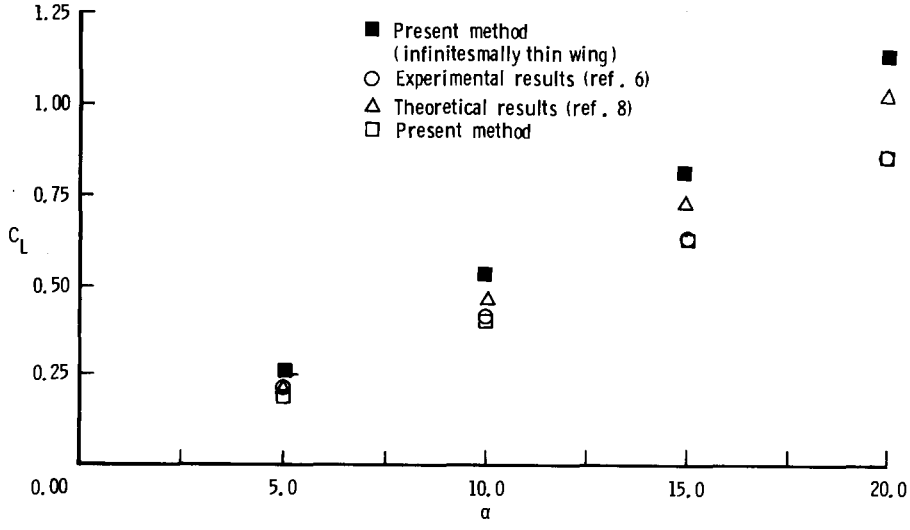

Fig. 5. Lift coefficients for a NACA 0012 section wing of $AR = 4/\sqrt{3}$.

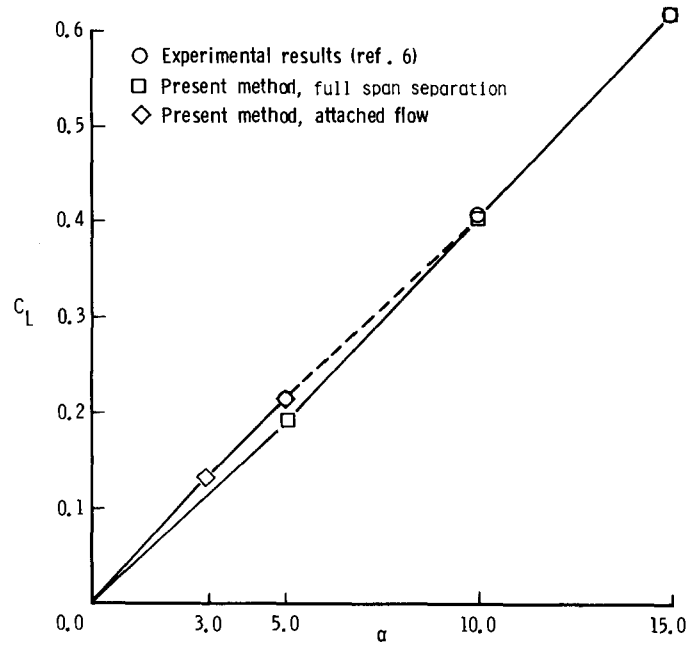

Fig. 6. Lift coefficients for a NACA 0012 section delta wing of $AR = 4/\sqrt{3}$ at small angles of attack.

angles of attack and at very low angles of attack the flow can be considered to be attached in the leading-edge region but we still have a nonlinear trailing wake. A perturbation theory is developed here to treat such an attached-flow situation in which both angle of attack and the thickness parameter are small. The mathematical formulation of this problem is given in Appendix A.

Lift coefficients are obtained for the NACA 0012 section wing of $AR = 4/\sqrt{3}$ at low angles of attack with the assumption of attached flow at the leading edge and a nonlinear wake issuing from the trailing edge. They are presented in Fig. 6. In the figure, the lift coefficient obtained by the present method and by experiments [6] at 5°, 10°, and 15° of angles of attack are shown. The branch of the lift curve obtained with the assumption of attached flow near the leading edge seems to have a higher gradient than the main lift curve corresponding to higher angles of attack. The lift coefficient obtained at 5° with the assumption of attached flow near the leading edge seems to be in fairly good agreement with the experimental results, whereas the lift coefficient obtained with the assumption of the full-span leading-edge vortex flow falls below the experimental results at 5°. This shows that for a round-edged delta wing at low angles of attack (until about 5°) the flow is such that we can assume an attached flow at the leading edge and get good estimates of the lift coefficients. At higher angles of attack (above 10°) we have full-span leading-edge separation and the present model predicts the lift coefficients very well. In the intermediate range (i.e., 5°–10°) it would appear that there is part-span leading-edge separation which is not predicted by the present model or by the attached-flow theory. To get a good estimate in this region part-span separation has to be built into the numerical model.

4.5. Conclusions

A perturbation theory is developed to treat the effects of thickness on the lift of low-aspect-ratio delta wings in incompressible flow at moderate angles of attack. The problem has been split

into basic and first-order components and the solution procedures are described. The effects of the nonlinear nature of the leading-edge vortex sheet and the trailing-edge sheet are pointed out. It is shown that the first-order lifting problem has to be solved together with the basic problem.

The first-order problem of flow over a delta wing with thickness is solved by the nonlinear discrete-vortex-segment method. The lifting elements of the flow are modeled by the vortex segments and the thickness elements are modeled by constant-strength source panels. Results are obtained for a sharp biconvex wing and a NACA 0012 section at higher angles of attack. The important observation that the effect of thickness is to decrease the lift is made.

A theory based on perturbation analysis is developed to obtain the aerodynamic characteristics of delta wings with round leading edges at small angles of attack. It is shown that at very low angles of attack it is necessary to assume attached flow near the leading edges of these round-leading-edge wings to get good estimates of the lift coefficients. The range of angle of attack at which part-span separation may occur is also indicated.

Acknowledgements

This work was supported by NASA Langley Research Center under Grant NCC1-41. The authors thank the Computer Science Center of the University of Maryland for supplying computer time.

Appendix A

Mathematical formulation for wings with round leading edges at small angles of attack

Consider again the steady incompressible inviscid flow of a uniform stream of speed U at angle of attack α past a delta wing with thickness. The thickness parameter τ as well as the angle α are assumed to be very small and we take $\alpha = O(\tau)$. The problem is treated as before except now the flow is assumed to be attached along the leading edge and only the trailing-edge wake needs to be modeled. An expansion in both α and τ is made and the approach parallels the work of Weber [22].

An outline of the mathematical formulation follows. We will highlight the aspects which differ from the formulation developed for moderate angles of attack. Details can be found in Dodbele [26].

The velocity potential is written as

$$\Phi = Ux - \frac{U\alpha^2 x}{2} + U\alpha z + \phi \tag{A1}$$

where ϕ is the disturbance velocity potential. For small α and τ, ϕ is expanded as

$$\phi = \tau\phi_{1\tau} + \alpha\phi_{1\alpha} + \alpha\tau\phi_{\alpha\tau} + \alpha^2\phi_{2\alpha} + \tau^2\phi_{2\tau} + O(\alpha^3, \tau^3, \alpha\tau^2, \tau\alpha^2). \tag{A2}$$

The first and second-order wing boundary conditions (corresponding to equations (14) and (15)) are:
first order:

$$\mp\tau UZ_{tx} + U\alpha + \alpha\phi_{1\alpha z}(x, y, 0\pm) + \tau\phi_{1\tau z}(x, y, 0\pm) = 0; \tag{A3}$$

second order:

$$\alpha\tau\left[\mp Z_{tx}\phi_{1\alpha x}(x, y, 0\pm) \mp Z_{ty}\phi_{1\alpha y}(x, y, 0\pm) \pm Z_t\phi_{1\alpha zz}(x, y, 0\pm)\right]$$

$$+\tau^2\left[\mp Z_{tx}\phi_{1\tau x}(x, y, 0\pm) \mp Z_{ty}\phi_{1\tau y}(x, y, 0\pm) \pm Z_t\phi_{1\tau zz}(x, y, 0\pm)\right]$$

$$+\alpha\tau\phi_{\alpha\tau z}(x, y, 0\pm) + \alpha^2\phi_{2\alpha z}(x, y, 0\pm) + \tau^2\phi_{2\tau z}(x, y, 0\pm) = 0. \tag{A4}$$

The wing boundary conditions for the first-order lifting and thickness problems, respectively, are obtained from equation (A3) as

$$\phi_{1\alpha z}(x, y, 0\pm) = -U \tag{A5}$$

and

$$\phi_{1\tau z}(x, y, 0\pm) = \pm UZ_{tx}. \tag{A6}$$

The thickness and lifting problems are independent at first order. Also, $\phi_{1\alpha}$ is seen to represent the zero-thickness lifting problem for a delta wing with a nonlinear trailing wake. It is solved with the discrete vortex-lattice method. The first-order thickness problem is represented by a source sheet with source strength per unit area $2UZ_{tx}$.

The wing boundary conditions for the three second-order components are obtained from equation (A4) as

$$\phi_{2\alpha z}(x, y, 0\pm) = 0, \tag{A7}$$

$$\phi_{\alpha\tau z}(x, y, 0\pm) = \pm Z_{tx}\phi_{1\alpha x}(x, y, 0\pm) \pm Z_{ty}\phi_{1\alpha y}(x, y, 0\pm)$$

$$\mp Z_t\phi_{1\alpha zz}(x, y, 0\pm), \tag{A8}$$

$$\phi_{2\tau z}(x, y, 0\pm) = \pm\frac{\partial}{\partial x}\left[Z_t\phi_{1\tau x}(x, y, 0\pm)\right] \pm \frac{\partial}{\partial y}\left[Z_t\phi_{1\tau y}(x, y, 0\pm)\right]. \tag{A9}$$

where Laplace's equation was used to obtain equation (A9).

The lifting potential $\phi_{2\alpha}$ satisfies a homogeneous problem and is zero. The potential $\phi_{\alpha\tau}$ is a lifting potential and $\phi_{2\tau}$, the second-order thickness potential, satisfies a nonlifting problem. The contribution of the second-order thickness potential to the wing lift is negligible compared to the contribution of the first-order thickness potential and so its effect is neglected in the calculation.

The complete second-order lifting potential is

$$\phi_{2L} = \alpha\phi_{1\alpha} + \alpha\tau\phi_{\alpha\tau} \tag{A10}$$

and the second-order lifting problem must be solved along with the first-order lifting problem due to the presence of the nonlinear trailing-edge wake. Again, the discrete vortex-lattice method is used.

References

1. Bartlett, G.E. and Vidal, R.J.: Experimental investigation of influence of edge shape on the aerodynamic characteristics of low aspect ratio wings at low speeds, *Journal of the Aeronautical Sciences* 22 (1955) 517–533.
2. Peckham, D.H.: Low speed wind tunnel tests on a series of uncambered pointed wings with sharp edges, ARC R&M 3186 (1961).

3. Wentz, W.H. and McMahon, M.C.: An experimental investigation of the flow fields about delta and double delta wings at low speeds, NASA CR 521 (1966).
4. Wentz, W.H.: Effects of leading edge camber on low speed characteristics of slender delta wings, NASA CR 2002 (1972).
5. Hummel, D.: On the vortex formation over a slender wing at large angles of incidence, Paper No. 15, AGARD CP 247 (1979).
6. Jacquet, B.N. and Brewer, J.D.: Low speed static stability and rolling characteristics of low aspect ratio wings of triangular and modified triangular planforms, NACA RM No. L8L29 (1948).
7. Smith, J.H.B.: Inviscid fluid models, based on rolled-up vortex sheets, for three dimensional separation at high Reynolds number, Paper No. 9, AGARD LS 94 (1978).
8. Lamar, J.E. and Campbell, J.F.: Recent studies at NASA Langley of vortical flows interacting with neighboring surfaces, *AGARD Symposium on Vortical Type Flows*, Rotterdam, the Netherlands (1983).
9. Hoeijmakers, H.W.M.: Computational vortex flow aerodynamics, AGARD CP 342, Paper No. 18 (1983).
10. Polhamus, E.C.: A concept of the vortex lift of sharp edge delta wings based on a leading edge suction analogy, NASA TND-3767 (1966).
11. Lamar, J.E. and Gloss, B.B.: Subsonic aerodynamic characteristics of interacting lifting surfaces with separated flows around sharp edges predicted by a vortex lattice method, NASA TND-7921 (1975).
12. Lan, C.E. and Hsu, C.H.: Effects of vortex breakdown on longitudinal and lateral-directional aerodynamics of slender wings by the suction analogy. AIAA 82-1385 (1982).
13. Johnson, F.T., Tinoco, E.N., Lu, P. and Epton, M.A.: Three dimensional flow over wings with leading edge vortex separation, *AIAA Journal* 18 (1980) 367–380; also AIAA 79-0282 (1979).
14. Kandil, O.A., Mook, D.T. and Nayfeh, A.H.: Nonlinear prediction of aerodynamic loads on lifting surfaces, *Journal of Aircraft* 3 (1976) 22–28.
15. Kandil, O.A., Chu, L.C. and Yates, E.C.: Hybrid vortex method for lifting surfaces with free vortex flow, AIAA 80-0070 (1980).
16. Zorea, C.R. and Rom, J.: The calculation of nonlinear aerodynamic characteristics of wing and their wake in subsonic flow, *20th Israel Annual Conf. on Aviation and Astronautics* (1978) 36–48.
17. Gordon, R. and Rom, J.: Calculation of nonlinear subsonic characteristics of wings with thickness and camber at high incidence, *AIAA Journal* 23 (1985) 817–825.
18. Kulfan, R.M.: Wing airfoil shape effects on the development of leading edge vortices, AIAA 79-1675 (1979).
19. Lamar, J.E.: Private communication.
20. Manro, M.E.: Aeroelastic loads predicted for an arrow wing, NASA CR 3642 (1983).
21. Plotkin, A.: Thickness and camber effects in slender wing theory, *AIAA Journal* 21 (1983) 1755–1757.
22. Weber, J.: Second order small perturbation theory for finite wings in incompressible flows, ARC R&M 3759 (1972).
23. Sells, C.C.L.: Iterative methods for thick cambered wings in subcritical flow, ACR R&M 3786 (1974).
24. Ashley, H. and Landahl, M.T.: *Aerodynamics of Wings and Bodies*, Addison-Wesley Publishing Company, Inc., Massachusetts (1965).
25. Woodward, F.A.: An improved method for the aerodynamic analysis of wing-body-tail configurations in subsonic and supersonic flow, NASA CR-2228 (1973).
26. Dodbele, S.S.: Lift due to thickness for low aspect ratio wings in incompressible flow, Ph.D. Thesis, Dept. of Aerospace Engineering, University of Maryland (1984).
27. Dodbele, S.S. and Plotkin, A.: Lift due to thickness for low aspect ratio wings in incompressible flow, AIAA 85-1588 (1985).